Saudi Journal of Biological Sciences 26 (2019) 767–776

Contents lists available at ScienceDirect

Saudi Journal of Biological Sciences

journal homepage: www.sciencedirect.com

Original article

Mitochondrial dysfunction mediated apoptosis of HT-29 cells through CS-PAC-AgNPs and investigation of genotoxic effects in zebra (*Danio rerio*) fish model for drug delivery

Mani Suganya [a], Balasubramanian Mythili Gnanamangai [a], Chandramohan Govindasamy [b], Mohamed Farouk Elsadek [b], Arivalagan Pugazhendhi [c,*], Veeramani Chinnadurai [b], Arokiyaraj Selvaraj [d], Balasubramani Ravindran [e], Soon Woong Chang [e], Ponnusamy Ponmurugan [f,*]

[a] Department of Biotechnology, K. S. Rangasamy College of Technology, Tiruchengode 637215, Tamil Nadu, India
[b] Department of Community Health Sciences, College of Applied Medical Sciences, King Saud University, P.O. Box 10219, Riyadh 11433, Saudi Arabia
[c] Innovative Green Product Synthesis and Renewable Environment Development Research Group, Faculty of Environment and Labour Safety, Ton Duc Thang University, Ho Chi Minh City, Viet Nam
[d] Department of Food Science and Biotechnology, Sejong University, Seoul, Republic of Korea
[e] Department of Environmental Energy and Engineering, Kyonggi University, Youngtong –Gu, Suwon 16227, South Korea
[f] Department of Botany, Bharathiar University, Coimbatore 641 046, Tamil Nadu, India

ARTICLE INFO

Article history:
Received 15 January 2019
Revised 24 February 2019
Accepted 19 March 2019
Available online 20 March 2019

Keywords:
Proanthocyanidin
Characterization
Western blotting
in vivo (zebra fish) model

ABSTRACT

The present study reports the validation of cancer nanotherapy using proanthocyanidin (PAC). Nowadays, *in vitro* and *in vivo* deliveries of nanoparticle (NPs) drugs have been paid more attention, intensively. Moreover, the current chemotherapeutic drugs have few first rate drawbacks including lack of specificity and requirement of excessive drug doses. To overcome this problem of chemotherapy, the attainment of high drug loading in combination with degradable polymer nanoparticles (for instance,chitosan) is a trending research in cancer biology. Hence, in this study, the synthesized PAC-AgNPs were successfully crosslinked with chitosan nanoparticles (CS-PAC-AgNPs), which were found to be spherical or polygonal in shape with a median size of 70.68 nm and 52.16 nm as observed by FTIR, FESEM and TEM analysis; thus, being suitable for drug delivery. CS-PAC-AgNPs were taken up via endocytosis by cancer cells and enabled the release cytochrome-C from mitochondria, followed by dysregulation of anti-apoptotic protein Bcl2 family, inducing the apoptotic mediated activation of caspase 9 and 3. To identify the genotoxicity of the synthesized CS-PAC-AgNPs, the mortality, hatching rate, malformation and abnormalities of embryo/larvae of the vertebrate zebra fish model (*Danio rerio*) were observed in a dose-time-dependent manner. This improved cancer nanotherapy can thus be utilized as a novel nanocombination for inducing apoptosis *in vitro* and *in vivo*.

1. Introduction

Mitochondrial mediated proteins can damage the DNA or upregulated oncogenes when growth factor deprivation, high concentration of cytosolic Ca^{2+} and oxidative stress occur in Bcl2 family of proteins (Siegel et al., 2014; Bauer and Hefand, 2006; Lomonosova and Chinnadurai, 2008; Elmore, 2007; Hassan et al., 2014; Zaman et al., 2014). Drugs such as doxorubicin, paclitaxel, cisplatin and combination drugs had been extensively utilized in malignancy treatment (Berry, 2005). However, these operators have indicated sudden toxicities to healthy tissues and the patients would be afflicted by excessive element effects (Oh et al., 2007). In addition, most of the chemotherapeutic candidates might not kill most of the cancer cells and their repetitive administration develops drug resistance, which is even harder to deal with. Hence there is an earnest need to create remedial modalities with no or negligible reactions to healthy tissues (Urakami et al., 2008).

* Corresponding authors.
E-mail addresses: arivalagan.pugazhendhi@tdtu.edu.vn (A. Pugazhendhi), cancerbiology41@gmail.com (P. Ponmurugan).
Peer review under responsibility of King Saud University.

Production and hosting by Elsevier

https://doi.org/10.1016/j.sjbs.2019.03.007
1319-562X/

In this context, an assortment of characteristic nutritional compounds not much more effective for the targeted drugs, which have been investigated to conjugate the metal oxide and degradable nanoparticles for accurate drug delivery system. *In vitro* studies were carried out with novel CS-PAC-AgNPs for the ability to enhance the anticancer activities through a mitochondrial-mediated signaling pathway in HT-29 cells. To investigate the genotoxic effect on zebra fish embryo and larvae induced by CS-PAC-AgNPs, an arrangement evaluation, including embryonic mortality, hatching rate, distortion and entire embryo developing stage of cell death, were performed. Thus, the current approach could provide a platform to design/develop anticancer drug delivery system, especially for colon cancer.

2. Materials and methods

2.1. Synthesis of chitosan coated PAC- AgNPs

The detailed preparation of the nanoparticles from chitosan coated materials were reported in our previous study (Mani et al., 2019). The bioactive compound loaded with chitosan nanoparticles (CS-PAC-AgNPs) was prepared by the nanoprecipitation technique (Venkatachalam et al., 2016). Fig. 1 represents the preparation method for PAC-AgNPs. Chitosan coated PAC-AgNPs (positive charge) were interacting with a TTP (negative charge) solution by a convenient ionic gelation technique.

2.2. Nanoparticle characterization

Fourier transform infrared spectroscopy (FTIR) investigation of chitosan coated PAC-AgNPs were documented by a PerkinElmer FTIR 4000 spectrometer. The surface morphology of the NPs was examined by FESEM (FEI Nova Nano 600, Netherlands and TEM, Tecnai G20, FEI Company, Hillsboro, OR).

2.3. Cell culture

Human Colorectal cancer (HT-29) cell line was grown in RPMI-1640 medium (Gibco-BRL) containing 10% v/v warm-suspended fetal bovine serum (Gibco-BRL) with 2 mM-glutamine (Sigma Chemical), penicillin (100 mg/mL) and streptomycin (100 mg/mL). These supplemented media are referred as complete media or growth media and cells were passaged regularly and subcultured in 90% confluence with 0.2% trypsin (w/v) for every 2–3 days.

2.4. MTT cell viability and morphometric analysis assay

The anchorage dependent cell viability of HT-29 cells treated with CS-PAC-AgNPs was assessed using cytotoxic assay (Ana et al., 2018). The experiment for morphometric analysis was performed by following the method of Kavitha et al. (2018).

2.5. Calcein – AM/EH staining

The cell death induced by nanoparticles, which is based on the difference in membrane integrity between the live and dead cells, was measured (Erlei et al., 2017).

2.6. DAPI staining

DAPI is a blue fluorescent dye that is sensitive to chromatins and very less toxic to cells; it can be employed to observe the nuclei changes in apoptotic cells. The images of the stained cells were captured using a fluorescence microscope with a suitable excitation filter (Vivek et al., 2012).

2.7. DNA fragmentation and cell apoptosis analysis

For both the analyses, the reported methodologies of Karthi et al. (2016) and Mathangi et al. (2015) were followed.

2.8. Western blotting

The cells were treated for 24 h with respective GI_{50}convergences of PAC-AgNPs and CS-PAC-AgNPs for the induction of apoptosis (Tao et al., 2017).

2.9. In-vivo studies

2.9.1. Parental fish growth and egg placement

The zebra fish, utilized as spawners, had a length of 3.62 cm and a weight of 1.00 gm. Prior to spawning, the male and female fish were housed independently for atleast 10 days. Care was taken in gathering the eggs. The glass tank secured with a fine nylon internet with an appropriate fitting crosssection estimate for eggs to fall through, were put in the aquarium on the day before breeding; male and female fish were taken in the ratio of 2:1 (male:female) to get the maximum quantity of embryos. The collected embryos were treated with various concentrations (1.56–25 μg/mL) of PAC, PAC-AgNPs and CS-PAC-AgNPs for 24, 48 and 72 hpf of exposure, respectively under a stereomicroscope (Magnus MLX) at 10X and 40X magnifications.

2.9.2. Quantification of intracellular ROS level

The fertilized and healthy grown larvae were seeded in 6-well plates containing 5 mL of E3 medium. The drug optimized concentration of the synthesized PAC-AgNPs and CS-PAC-AgNPs was used to treat the larvae for 120 h. After incubation, the larvae were washed with PBS. The intracellular ROS level was measured using 10 μM H_2-DCFDA stain after incubation for 30 min in dark. The ROS discharge was checked by using the transformation of non-fluorescent H_2-DCFDA into highly fluorescent 2′,7′- dichlorofluorescein (DCF), utilizing a stereofluorescence microscope (Perkin Elmer, USA) with an excitation filter at 485-530 nm.

2.10. Statistical analysis

All the statistical analyses were carried out with SPSS version 20 for Windows. The entire data were communicated as mean ± SE of triplicate independent analysis. One-path ANOVA with Dunnett's post hoc test was used for multi-gather correlations (apart from the GI_{50} values, which were assessed by nonlinear regression examinations).

3. Results and discussion

3.1. Characterization of CS-PAC-AgNPs

FTIR spectroscopy was executed using KBr as a reference to show the characteristic peak of the PAC-AgNPs and CS-PAC-AgNPs nanocombination. The sharp absorption peaks at 3454.26 amines indiacted N—H stretching, the one at 2924.04 cm^{-1} represented the C—H stretching, vibration (alkanes), and those at 1632.41, 1384.43, 1261.31, 1021.26, 801.58 and 618.54 cm^{-1} could be designated to C=C (alkenes), C—H bend scissoring, C—O and C—H bending (Aromatic) in PAC-AgNPs (Fig. 2a). Moreover, CS-PAC-AgNPs have exhibited a strong transmittance peaks at 3835.50 (OH stretching of phenol), 3777.61 (NH_2 stretching of amines), 3417.37 (N—H stretching of amide), 2351.01 (C—H stretching (alkyl)), 2144.37 to 1641.38 (C=C and C=C medium, stretching vibration (alkyne)), 1192.78 (C—N stretching (Amines)), 1100.15–

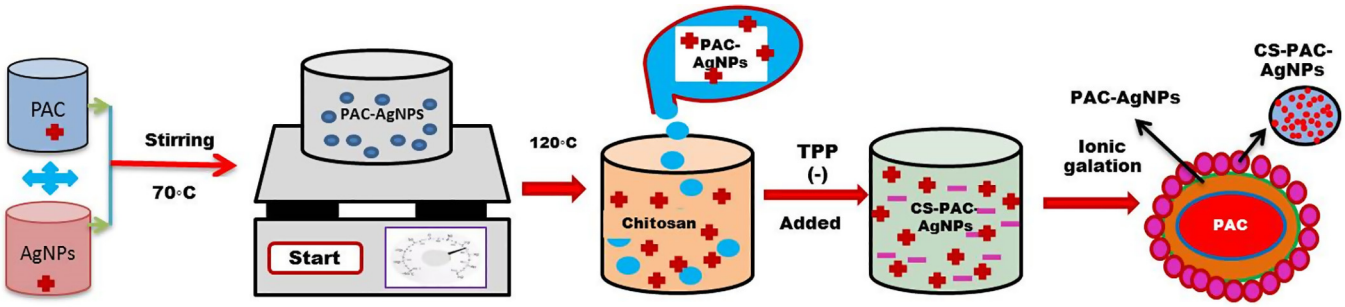

Fig. 1. Schematic represents the preparation method for PAC-AgNPs. Chitosan coated PAC-AgNPs (positive charge) were interacting with a TTP (negative charge) solution by a convenient ionic gelation technique.

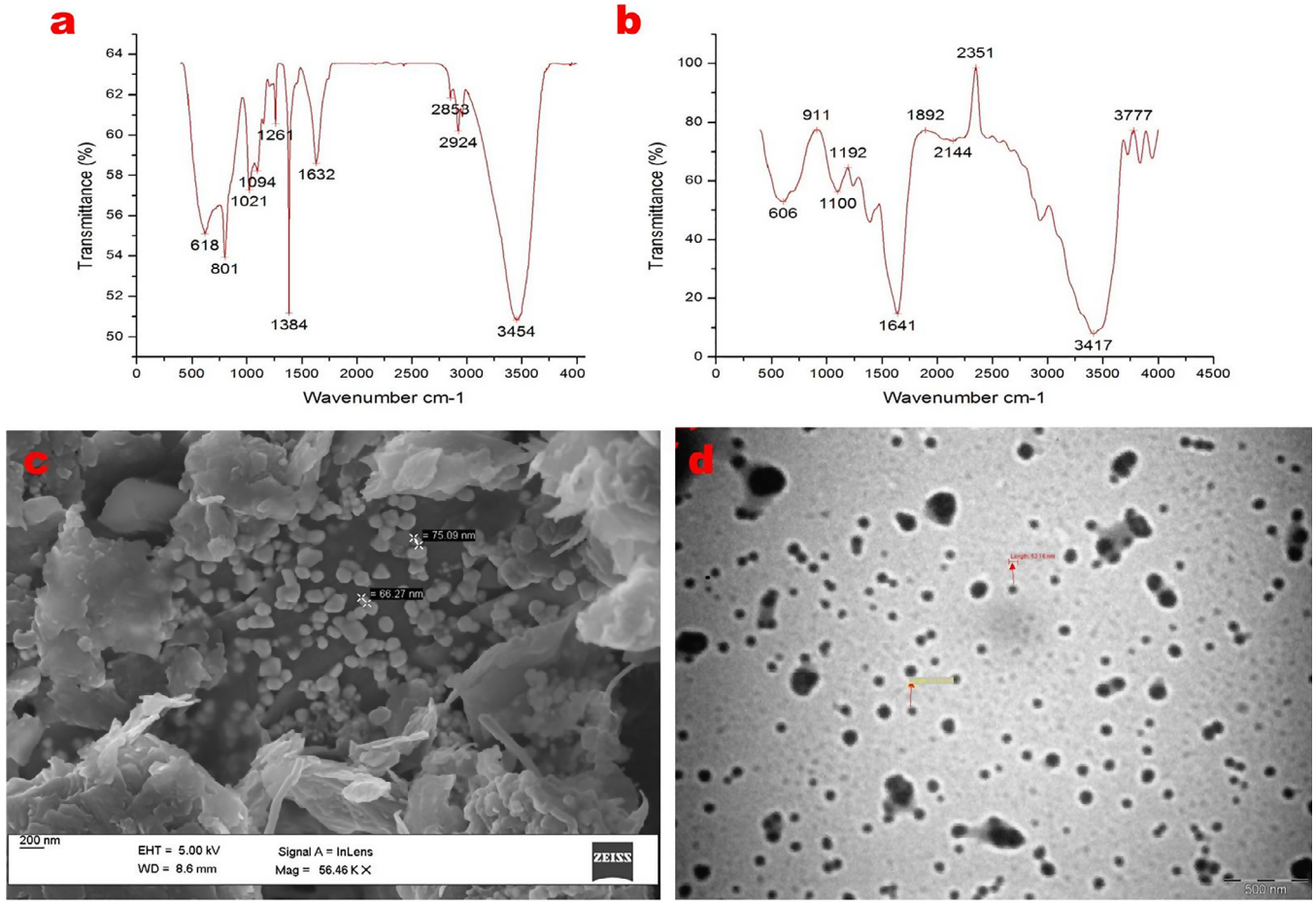

Fig. 2. Characterization of CS-PAC-AgNPs. (a) FTIR spectrum of PAC-AgNPs, (b) CS-PAC-AgNPs, (c) FE-SEM of synthesized PAC-AgNPs and (d) TEM image of CS-PAC-AgNPs.

606.9 (N—H and C—H bending), respectively. Similar peaks at 3417.37, 1641.38, 1192.78 and 606.96 cm^{-1} indicated the functional groups such as O—H stretching of the phenol, N—H expanding vibration of the amines, C—H and C=C stretching of the alkanes representing that CS was conjugated to the PAC-AgNPs of the synthesized samples, as shown in Fig. 2b. In the nanoformulation attributes, peak was discovered due to the capability interaction of protonated amide/amine gatherings and adversely charged TPP cross connecting specialist. Comparative functional groups for chitosan-covered iron oxide nanoparticles have been additionally pronounced (Unsoy et al., 2012). These observations strongly recommended that chitosan nanoparticles have been effectively loaded with PAC-AgNPs atoms via ionic interactions by means of the nanoprecipitation technique.

The exterior characteristics and the topological complexity of the PAC-AgNPs and CS-PAC-AgNPs were inspected utilizing a transmission electron magnifying lens. The perceptions from FESEM and TEM data yielded information on the molecule shapes and the assurance of particle sizes. The formed PAC-AgNPs (Fig. 2c) exhibited a spherical shape, smooth surface and uniform size distribution ranging from 70.68 nm whereas, the CS-PAC-AgNPs size range was between of 52.16 nm and a combination of exceptional single particles with clean becoming a member of barriers changed into round along side the normal geometry of the proximate polyhedron (pentagon and hexagen) formed particles (Fig. 2d). Spherical shaped particles, which are 100–200 nm in size, had the very best capacity for the extended movement; quickly and consistently disguised on account of their symmetry (Petros

and Desimone, 2010; Udompornmongkol and Chiang, 2016; Wang et al., 2015).

3.2. In vitro biological applications

3.2.1. Cytotoxicity assay

MTT assay is a commonly used technique to explore the cytotoxic impact of the synthesized nanoparticles. This examination depended on the capacity of the mitochondrial dehydrogenase enzymes from live cells to sever the tetrazolium rings of the light yellow MTT and frame dim blue formazan precious crystals, which would be mostly impermeable to cell membranes, bringing about its aggregation inside healthy cells. The cells had been treated with exceptional concentrations (1.52–25 μg/mL) of PAC, PAC-AgNPs and CS-PAC-AgNPs for 24 h (Fig. 3). However, the cell growth was substantially decreased while exposed to CS-PAC-NPs within the concentration range of 3.12 μg/mL. Futhermore, CS-PAC-NPs reduced cell growth potently in short times and in a concentration dependent way. In this case, it could be associated that CS-PAC-NPs had great anticancer activities. CS nanoparticles have derived an awesome application in nanomedicine because of their exclusive properties with the apparent therapeutic ability in finding and treating malignant tumors (Shukla et al., 2005; Naahidi et al., 2013; Arasu et al., 2013; Arokiyaraj et al., 2015; Valsalam et al., 2019).

3.2.2. Morphometric analysis

The morphometric changes were noticed in PAC, PAC-AgNPs and CS-PAC-AgNPs tested at a cytotoxicity inducing experimental GI_{50}concentration (3.25 μg/mL), against HT-29 cells. Untreated cells appeared normal, healthy to be elongated, forming confluent cells and attaching to the flask. In contrast, important changes in the morphology and density of cells were observed after treatment with the PAC compound alone for 24 h in a dose dependent manner. Meanwhile, PAC-AgNPs brought about greater biocompatibility such as cell size reduction, cells appearing rounded and membrane blebbing as shown in Fig. 4 and CS-PAC-AgNPs resulted in greater morphological changes (Anitha et al., 2014a, 2014b).

3.2.3. Calcein – AM/EH staining

Apoptosis, also known as programmed cell death, is regular to every multicellular living being for taking out cells by means of a complex however the exceedingly characterized program (You et al., 2017; Moumita et al., 2012). The live and dead cells have been observed by means of a fluorescence microscope. Optical images confirmed that the PAC-AgNPs and CS-PAC-AgNPs gradually decreased the range and density of cell growth based on GI_{50} concentration. Incubation of HT-29 cells treated with CS-PAC-AgNPs has drastically reduced the live cells binding with calcein (green) and increased the number of dead cells as observed with EH (red), correlated with the lowest attention and untreated groups (Fig. 4). The images clearly demonstrated the presence of apoptotic cells, such as irregular cells and formation of apoptotic bodies.

3.2.4. Fluorescence microscopic studies of nuclear staining

The apoptotic cell death is one of the mechanisms by which cell growth is extinguished. The cell nuclei were subsequently stained using DAPI. DAPI is a fluorescence stain that binds strongly to DNA. DAPI staining has been used to characterize the effects of CS-PAC-AgNPs induced apoptosis in cancer cells. Apoptosis is typically described by morphological and biochemical changes (Inoue and Tani, 2014). such as cytoplasmic shrinkage, nuclear chromatin condensation, shrinkage of nuclei, membrane blebbing and dilated endoplasmic reticulum. However, on treatment with PAC-AgNPs and CS-PAC-AgNPs, there was a significant nuclei fragmentation

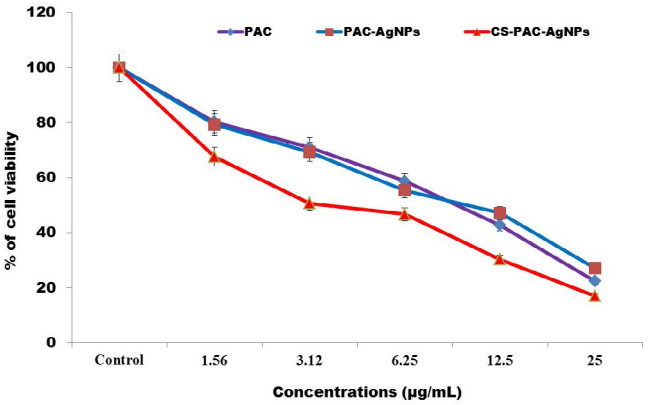

Fig. 3. Cytotoxic effects of CS-PAC-AgNPs exerted against Colon cancer (HT-29) cells. Cells were treated with different concentrations of (1.56–25 μg/mL)for 24 h. Cell reasonability was distinguished by MTT assay. The trials were done in triplicates and each value represents mean ± SE.

with condensed and apoptotic nuclei; when the incubation time was kept at 24 h, the number of apoptotic cells increased as shown in Fig. 4. Similar reports have shown that AgNPs could also induce DNA damage and apoptosis in cancer cells (Liu et al., 2017).

3.3. Biochemical changes in apoptosis

DNA fragmentation was accomplished to analyse the effective consequences of CS-PAC-AgNPs on cell dependability and DNA replication. No ladder formation was observed in untreated cells. In shorter incubation times, the PAC-AgNPs and CS-PAC-AgNPs achieved early apoptosis. When incubated for long term durations, the later phase apoptotic cells with more nuclear fragmentations were determined (Fig. 5) (Galluzi et al., 2007; Zheng et al., 2016).

3.4. Flow cytometry analysis

The effects of CS-PAC-AgNPs on apoptosis of HT-29 cells were determined by using annexin V/PI staining based on FACS analysis. Number of late and early apoptotic cells (6.30% and 28.50% in GI_{50} concentration of PAC; 5.50% and 39.6% in GI_{50} concentration of PAC-AgNPs; 8.80% and 56.4% in GI_{50} concentration of CS-PAC-AgNPs respectively) and necrotic cells (0.9% PAC, 0.3% PAC-AgNPs and 1.0% CS-PAC-AgNPs) were evaluated in comparison to untreated control cells (Fig. 6) (Getts et al., 2014; Wong, 2011; Chaudhari et al., 2012).

3.5. Western blotting

The HT-29 cells were treated with GI_{50} concentration (3.5 μg/mL) of PAC-AgNPs and CS-PAC-AgNPs for 24 h. The results disclosed important upregulation of the expression of Bax (pro-apoptotic protein) while the expressions of Bcl2 and Bcl-XL (anti-apoptotic protein) have been significantly downregulated, as delineated in Fig. 7. The CS-PAC-AgNPs significantly decreased the intensity of band ratio when compared to PAC-AgNPs. β-actin was utilized as a stacking control, which indicated measure up to equal intensity band and protein concentration in all examples. The induction of apoptosis initiated by medicate stacked chitosan nanoparticles was accounted (Vivek et al., 2013; Rowinsky, 2005).

Cytochrome C is a major constituent of intrinsic cell apoptotic signal molecules, which can initiate the caspase cascade reaction and induce apoptosis. The protein expression of cytochrome c releasing mitochondria in HT-29 cells was significantly downregulated when treated with CS-PAC-AgNPs for 24 h has been shown in

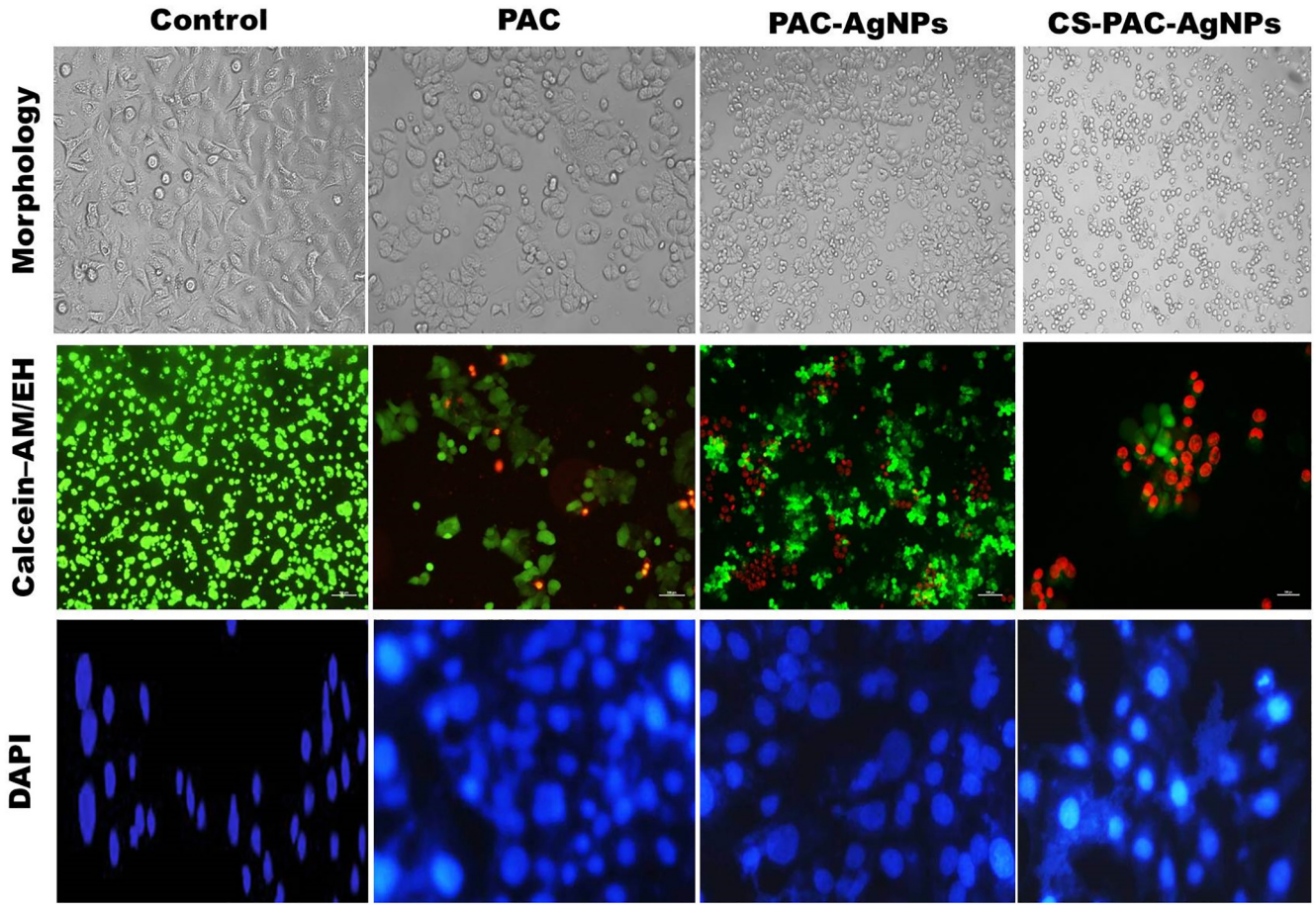

Fig. 4. Morphological characterization of HT-29 cells treated with GI_{50} concentration of 3.25 μg/mL of CS-PAC-AgNPs for 24 h.

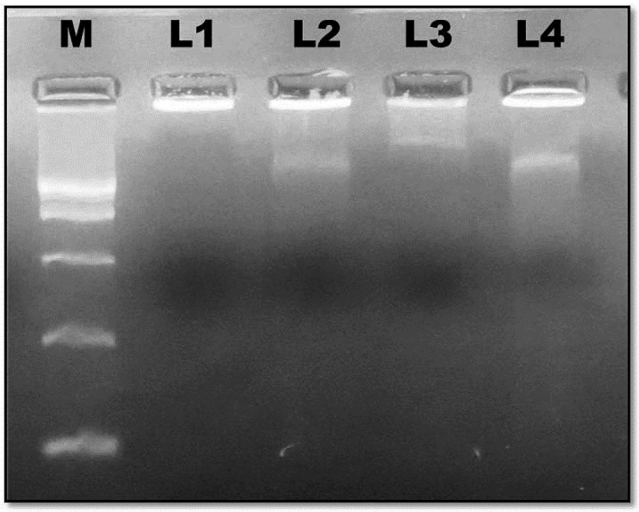

Fig. 5. Biochemical changes of apoptosis in HT-29 cells initiated by CS-PAC-AgNPs for 24 h. DNA fragmentation was evaluated by 1.5% agarose gel electrophoresis and ethidium bromide staining and viewed under a UV transilluminator. Fragmented internucleosomal DNA appears as a ladder. "M" indicates 1 bp DNA ladder; (L1) Control, (L2) PAC, (L3) PAC-AgNPs and (L4) CS-PAC-AgNPs.

Fig. 8. The initiator caspase - 9 at that point cuts and actuates the killer caspase - 3, 6 and 7, resulting in cell apoptosis (Loreto et al., 2011; Ghobrial et al., 2005).

The signal transduction of apoptotic key pathways occurred in caspase cascade reaction. The expressions of cellular apoptotic proteins, caspase - 9 and caspase - 3 were determined. The caspase enzyme to cleave the procaspase 9 and caspase 3, were found the up and down regulation process after treatment of CS-PAC-AgNPs as represented in Fig. 8 (Baig et al., 2016; Lee et al., 2007). Fig. 9 illustrates the overall possible mechanism of CS-PAC-AgNPs induced mitochondrial apoptosis signaling pathway.

3.6. In vivo studies

Zebra fish (*Danio rerio*) has been extensively used in biological and biochemical studies for checking out the genotoxic consequences. Zebra fish is an excellent animal model for *in vivo* imaging and biocompatability assessments of nanomaterials because of its high transparency, quicker embryonic development, smooth renovation and similarity with mammals viz. mice, rats and humans (Liu et al., 2012; Sreedevi et al., 2014; Hu et al., 2011).

3.7. Mortality and hatching rate

To assess the viable toxicities of PAC, PAC-AgNPs and CS-PAC-AgNPs (1.5–25 μg/mL) to zebra fish embryos, the death and hatching rates were assessed during a continuing observation period. This was done by counting live/dead embryos and larvae in each of the exposure chambers. At lower concentrations there was no extensive difference in mortality. At higher concentrations of 12.5–25 μg/mL, the mortality rate was increased significantly compared to the control. The hatching period of 48–72 hpf was the normal incubation time of embryos. Fig. 10 demonstrates a strong inhibition of hatching rate by CS-PAC-AgNPs. At 72 hpf, the hatch-

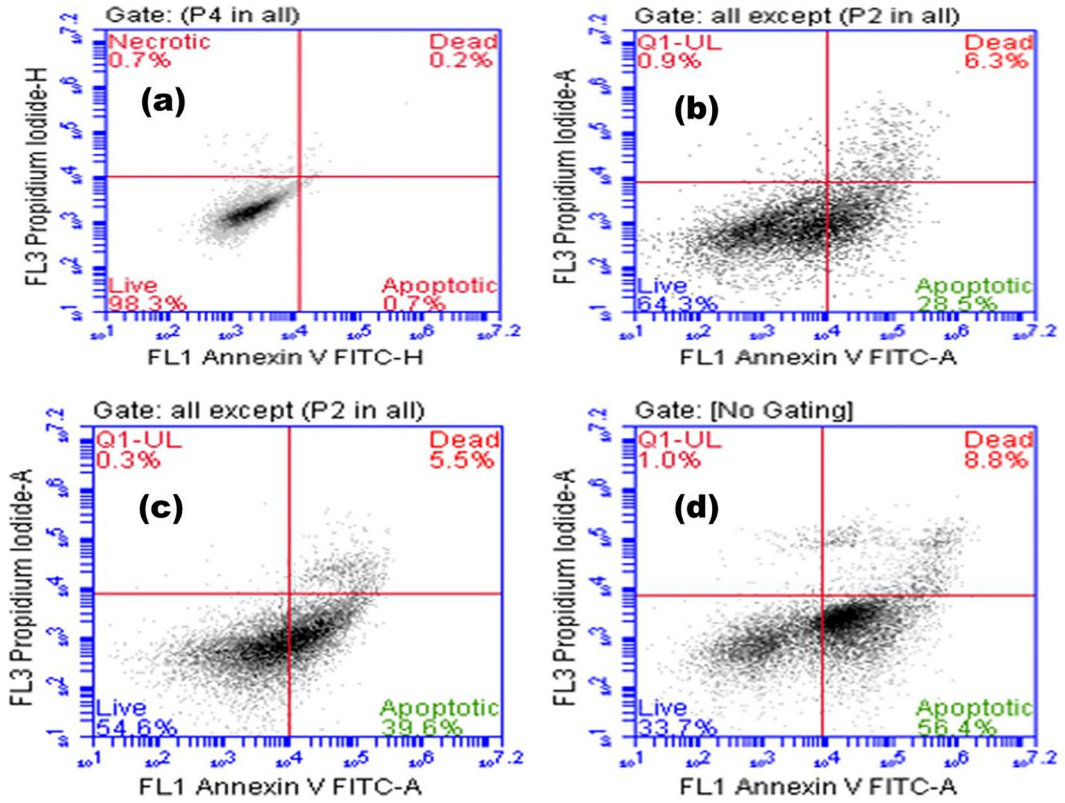

Fig. 6. Apoptotic cell death in HT-29 cells induced by CS-PAC-AgNPs as detected by flow cytometry. (a) Control, (b) PAC, (c) PAC-AgNPs and (d) CS-PAC-AgNPs.

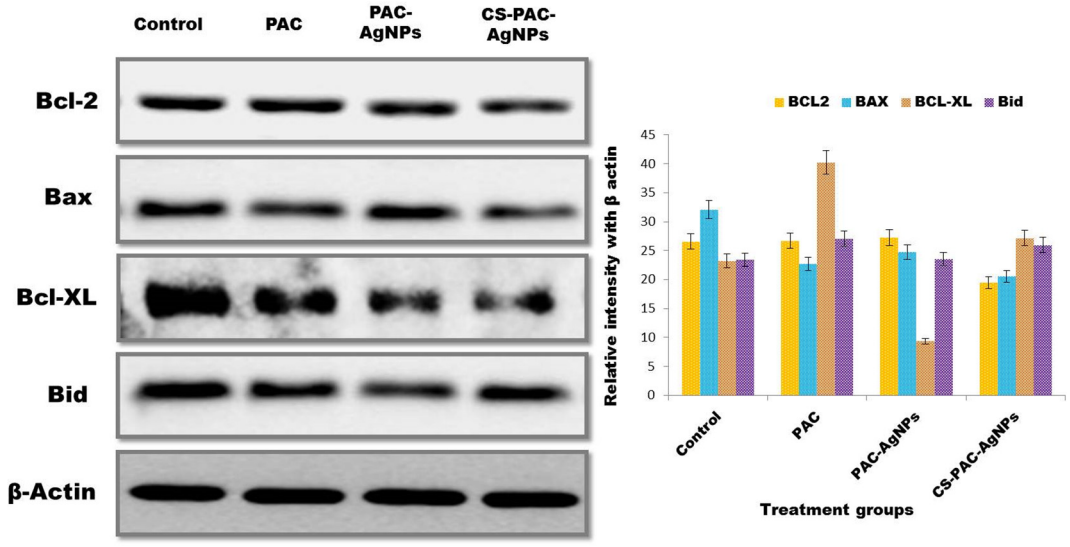

Fig. 7. Expression of apoptosis related proteins in HT-29 cells, induced by CS-PAC-AgNPs for 24 h as confirmed by western blot analysis.

ing rate at 25 μg/mL concentration (25.0%) was less than the control (95.0%) (Fig. 11). The improved measurements was persisted for further studies (3.25 μg/mL).

3.8. ROS generation

The capacity of CS-PAC-AgNPs to initiate oxidative stress was distinguished by the utilization of non-fluoresence dye 2,7-dichlorofluorescin diacetate (H_2-DCFDA). The aggregation of ROS outcomes in the oxidation of H_2-DCF stain treated larvae exhibited excessive green fluorescence intensity when compared to the untreated larvae in a concentration and time dependent manner as shown in Fig. 12. Moreover, a low level of fluorescence was emitted by PAC whereas the particles covered with metal and polymeric naoparticles have discharged a high intensity of fluorescence. Oxidative stress has been proposed to be one of the mechanisms of cell death, induced by using most of the metal oxide nanoparticles (Stone and Donaldson, 2006). Oxidative stress ensues as a consequence of imbalance between the generation of ROS and cancer prevention in the biological system. In this inves-

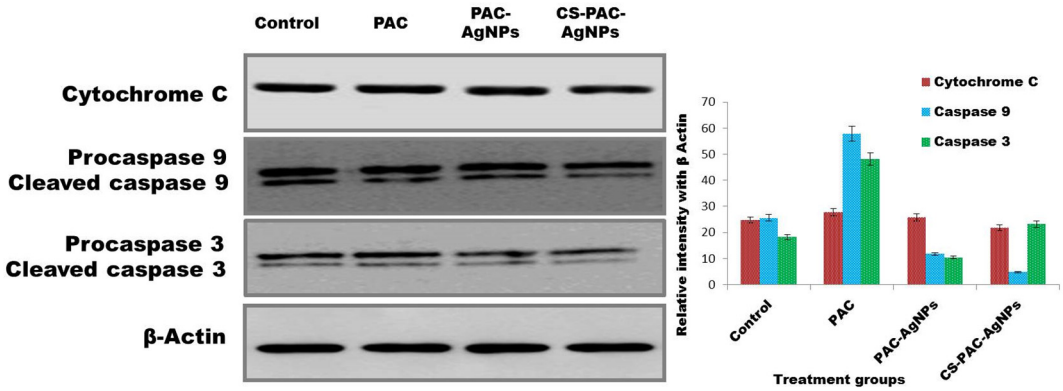

Fig. 8. Activation of caspase-dependent apoptotic pathway in HT-29 cells, treated with CS-PAC-AgNPs for 24 h as confirmed by western blot analysis.

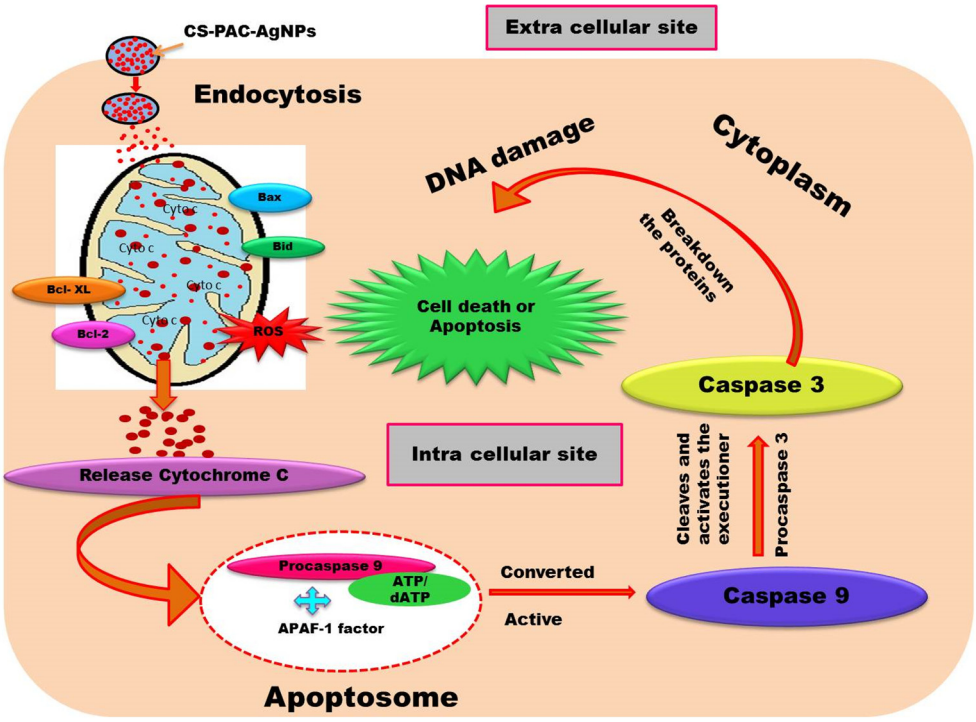

Fig. 9. Overall possible mechanism of CS-PAC-AgNPs induced mitochondrial apoptotic signaling pathway.

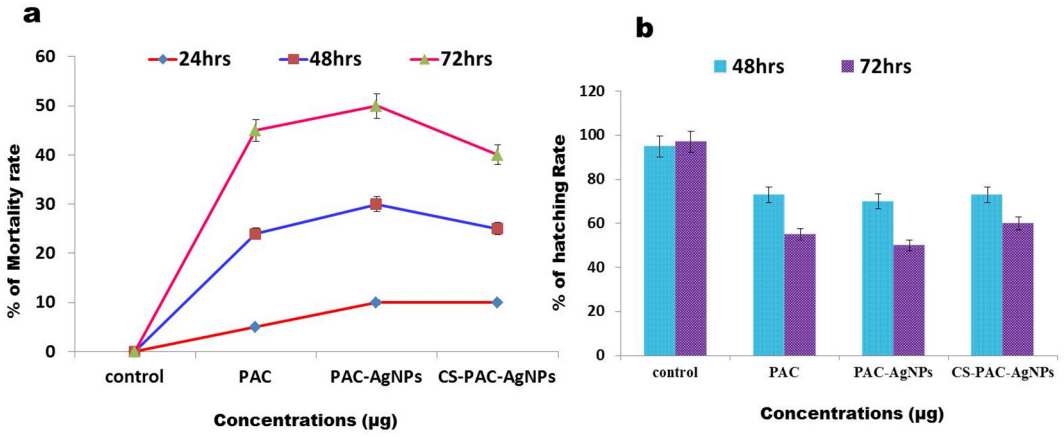

Fig. 10. Mortality and hatching rate of zebrafish embryos exposed to CS-PAC-AgNPs increased in a dose-and time-dependent manner. Data are presented as mean ± S.E of three independent tests. (a) Percentage of mortality rate and (b) percentage of hatching rate.

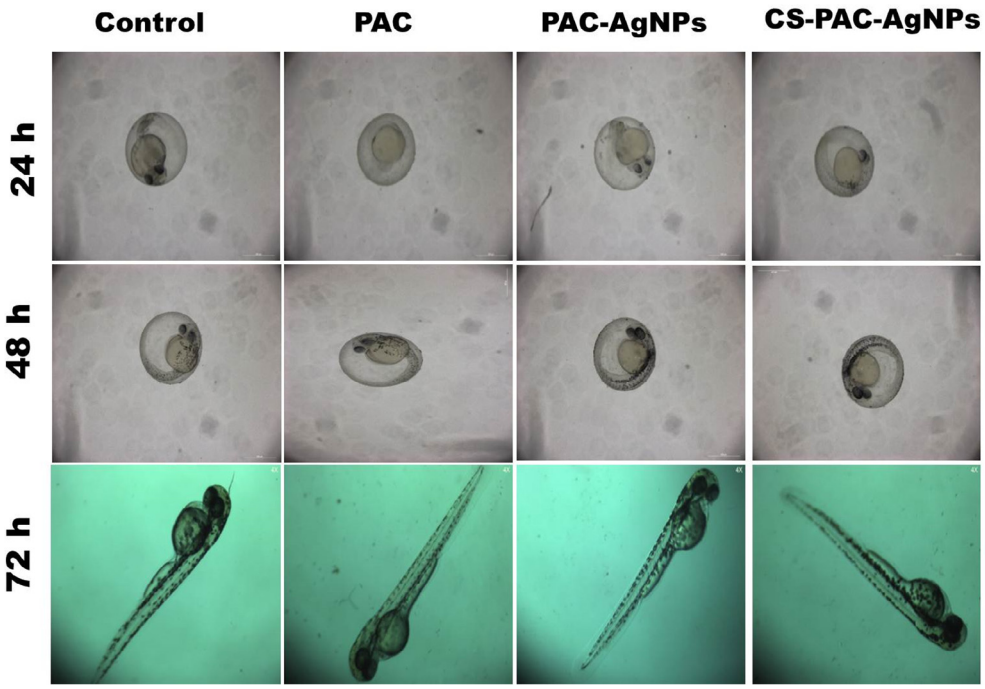

Fig. 11. Representative images of genotoxic effects in zebrafish embryo and larvae based on different incubation hours post fertilization (hpf).

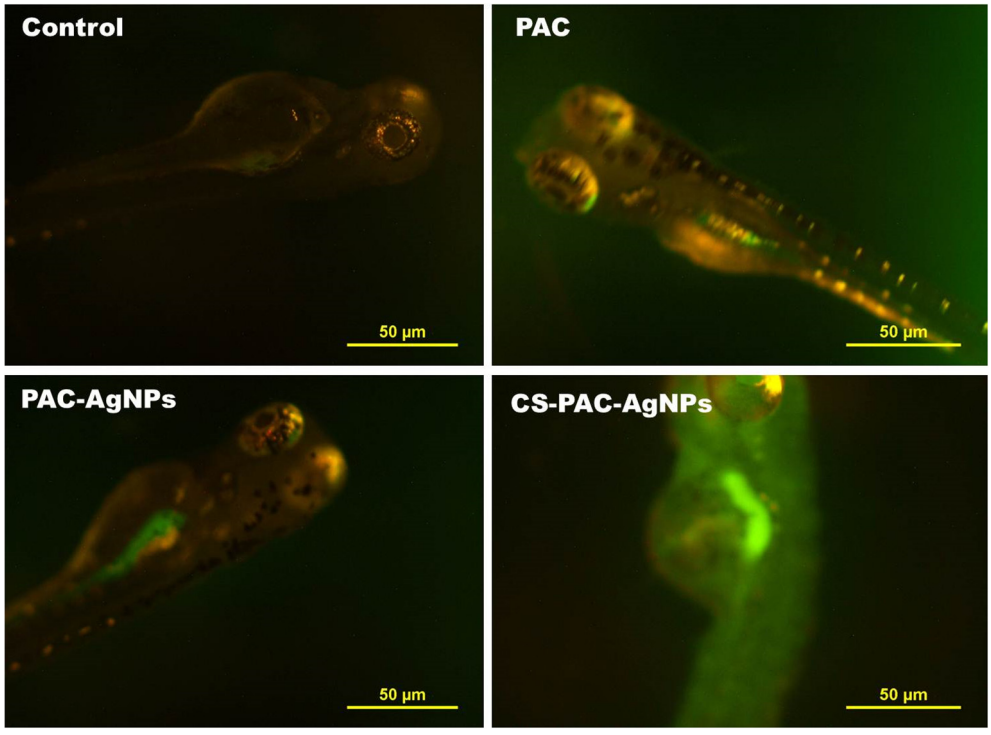

Fig. 12. Fluorescent microscopic images of ROS in zebrafish larvaes following exposure to CS-PAC-AgNPs for 120 h.

tigation, it was determined that CS-PAC-AgNPs, even at a low concentration, caused ROS generation. Subsequently, it has been deliberated that ROS generation in the present setting might be a definitive reason for cell death in larvae, acting through DNA damage, genomic instability, loss of cell membrane and cell death (Jezek and Hlavata, 2005; Sandeep and Pandey, 2014).

4. Conclusions

In summary, a novel nanocombination using biodegradable chitosan has been synthesized to improve biocompatability, low toxicity and solubility of the drugs. In particular, this drug was found to enhance the mortality of colon cancer cells with an underlying

molecular mechanism of intrinsic pathway. *In vivo* studies have used the developmental zebrafish model for assessing genotoxic effects of the synthesized CS-PAC-AgNPs. In conclusion, the new nanocombination in this study, may further advance the use of CS-PAC-AgNPs-based nanotherapeatic biomaterials, for various biomedical applications, especially cancer nanotherapy.

Conflict of interest

None declared conflict.

Acknowledgments

The authors gratefully acknowledge the DST-INSPIRE sponsored program, Department of Science and Technology, New Delhi (REF. NO: DST/INSPIRE Fellowship/2015/IF150459). The authors also acknowledge the Head, Department of Biotechnology, K. S. Rangasamy College of Technology for the support offered towards the study. The authors also acknowledge DST-FIST CSR/AST/College-233/2014 (fund for infrastructure for science and technology) and DBT–STAR (LBT/HRD/11/09/2018) for the support given to carry out the study. The authors would like to extend their sincere appreciation to the Deanship of Scientific Research at King Saud University for funding this Research (RG no - 1437-024). The authors are also grateful to the research collaboration among institutes and universities.

References

Ana, C.M.T., Diana, G.Z.T., Helen, Y.L.A., Andrea, A.A., Carolina, R.A., Cristina, R.P., 2018. Chitosan gold nanoparticles induce cell death in HeLa and MCF-7 cells through reactive oxygen species production. Int. J. Nanomed. 13, 3235–3250.

Anitha, A., Deepa, N., Chennazhi, K.P., Lakshmanan, V., Jayakumar, R., 2014a. Combinatorial anticancer effects of curcumin and 5-fluorouracil loaded thiolated chitosan nanoparticles towards colon cancer treatment. Biochim. Biophys. Acta 1840, 2730–2743.

Anitha, A., Sreeranganathan, M., Chennazhi, K.P., Lakshmanan, V.K., Jayakumar, R., 2014b. *In vitro* combinatorial anticancer effects of 5-fluorouracil and curcumin loaded N, O-carboxymethyl chitosan nanoparticles toward colon cancer and *in vivo* pharmacokinetic studies. Eur. J. Pharm. Biopharm. 88, 238–251.

Arasu, M.V., Duraipandiyan, V., Ignacimuthu, S., 2013. Antibacterial and antifungal activities of polyketide metabolite from marine Streptomyces sp. AP-123 and its cytotoxic effect. Chemosphere 90 (2), 479–487.

Arokiyaraj, S., Saravanan, M., Badathala, V., 2015. Green synthesis of silver nanoparticles using aqueous extract of Taraxacum officinale and its antimicrobial activity. South Indian J. Biol. Sci. 2, 115–118.

Baig, S., Seevasant, I., Mohamad, J., Mukheem, A., Huri, H.Z., Kamarul, T., 2016. Potential of apoptotic pathway – targeted cancer therapeutic research: where do we stand? Cell Death Dis. 7, e2058.

Bauer, J.H., Hefand, S.L., 2006. New tricks of an old molecule: lifespan regulation by p53. Aging Cell 5, 437–440.

Berry, W.R., 2005. The evolving role of chemotherapy in androgen-independent (hormone-refractory) prostate cancer. Urology 65, 2–7.

Chaudhari, K.R., Kumar, A., Megraj Khandelwal, V.K., Ukawala, M., Manjappa, A.S., Mishra, A.K., Monkkonen, J., Ramachandra Murthy, R.S., 2012. Bone metastasis targeting: a novel approach to reach bone using zoledronate anchored PLGA nanoparticle as a carrier system loaded with Docetaxel. J. Control. Rel. 158, 470–478.

Elmore, S., 2007. Apoptosis: a review of programmed cell death. Toxicol. Pathol. 35, 495–516.

Erlei, W., Yanjun, L., Caina, X., Jingbo, L., 2017. Antiproliferative and proapoptotic activities of anthocyanin and anthocyanidin extracts from blueberry fruits on B16–F10 melanoma cells. Food Nutr. Res. 61, 1–14.

Galluzi, L., Maiuri, M.C., Vitale, I., Zischka, H., Castedo, M., Zitvogel, L., Kroemer, G., 2007. Cell death modalities: classification and pathophysiological implications. Cell Death Differ. 14, 1237–1266.

Getts, D.R., Terry, R.L., Getts, M.T., Deffrasnes, C., Muller, M., Vreden, C., Ashhurst, T. M., Chami, B., Carthy, D.M., Wu, H., Ma, J., Martin, A., Shae, L.D., Witting, P., Kansas, G.S., Kuhn, J., Hafezi, W., Campbell, I.L., Reilly, D., Say, J., Brown, L., White, M.Y., Cordwell, S.J., Chadban, S.J., Thorp, E.B., Bao, S., Miller, S.D., King, N. J.C., 2014. Therapeutic inflammatory monocyte modulation using immune-modifying microparticles. Nanobiology 6, 219–227.

Ghobrial, I.M., Witzig, T.E., Adjei, A.A., 2005. Targeting apoptosis pathways in cancer therapy. CA Cancer J. Clin. 55, 178–194.

Hassan, M., Watari, H., Almaaty, A.A., Ohba, Y., Sakuragi, N., 2014. Apoptosis and molecular targeting therapy in cancer. BioMed Res. Int., 1–23

Hu, Y.L., Qi, W., Han, F., Shao, J.Z., Gao, J.Q., 2011. Toxicity evaluation of biodegradable chitosan nanoparticles using a zebra fish embryo model. Int. J. Nanomed. 6, 3351–3359.

Inoue, H., Tani, K., 2014. Multimodal immunogenic cancer cell death as a consequence of anticancer cytotoxic treatments. Cell Death Differ. 21, 39–49.

Jezek, P., Hlavata, L., 2005. Mitochondria in homeostasis of reactive oxygen species in cell, tissues, and organism. Int. J. Biochem. Cell Biol. 37, 2478–2503.

Karthi, N., Kalaiyarasu, T., Kandakumar, S., Mariyappan, P., Manju, V., 2016. Pelargonidin induces apoptosis and cell cycle arrest via mitochondria mediated intrinsic apoptotic pathway in HT-29 cells. RSC Adv. 6, 45064.

Kavitha, S., Suganya, M., Ponnusamy, P., Catherine, S.D.C., Matthew, L.D., Mythili, G. B., Sudhagar, P., 2018. Green-synthesis-derived CdS quantum dots using Tea leaf extract: antimicrobial, bioimaging, and therapeutic applications in lung cancer cells. ACS Appl. Nano Mater. 1, 1683–1693.

Lee, K.J., Nallathamby, P.D., Browning, L.M., Osgood, C.J., Xu, X.H.N., 2007. *In vivo* imaging of transport and biocompatibility of single silver nanoparticles in early development of zebra fish embryos. ACS Nano. 1, 133–143.

Liu, G., Yuan, Y., Long, M., Luo, T., Bian, J., Liu, X., Gu, J., Zou, H., Song, R., Wang, Y., Liu, Z., 2017. Beclin-1-mediated autophagy protects against cadmium-activated apoptosis via the Fas/FasL pathway in primary rat proximal tubular cell culture. Sci. Rep. 7, 977.

Liu, Y., Liu, B., Feng, D., Gao, C., Wu, M., He, N., Yang, X., Li, L., Feng, X., 2012. A progressive approach on zebra fish toward sensitive evaluation of nanoparticles toxicity. Integr. Biol. 4, 285–291.

Lomonosova, E., Chinnadurai, G., 2008. BH3-only proteins in apoptosis and beyond: an overview. Oncogene 27, S2–S19.

Loreto, C., Almeida, L.E., Trevilatto, P., Leonardi, R., 2011. Apoptosis in displaced temporomandibular joint disc with and without reduction: An immunohistochemical study. J. Oral Pathol. Med. 40, 103–110.

Mathangi, R., Shilpa, T., Ganga, B., Surabhi, R.P., Swetha, R., Prajisha, J., Jeyaraman, J., Suresh, K.R., Ganesh, V., 2015. Molecular mechanism of anti-cancer activity of phycocyanin in triple-negative breast cancer cells. BMC Cancer 15, 768.

Mani, S., Balasubramanian, M.G., Ponnusamy, P., et al., 2019. Antineoplastic effect of PAC capped silver nanoparticles promote apoptosis in HT-29 human colon cancer cells. J. Clust Sci. https://doi.org/10.1007/s10876-019-01510-1.

Moumita, G., Sourav, K., Mukhopadhyay, Sree Gayathri, Sandipan, B., Shrabani, B., Satyahari, D., Pradeep, N.D.S., 2012. Fluorene–morpholine-based organic nanoparticles: lysosometargeted pH-triggered two-photon photodynamic therapy with fluorescence switch on-off. J. Mater. Chem. B, 1–3.

Naahidi, S., Jafari, M., Edal, F., Raymond, K., Khademhosseini, A., Chen, P., 2013. Biocompatibility of engineered nanoparticles for drug delivery. J. Control. Rel. 166, 182–194.

Oh, W.K., Tay, M.H., Huang, J., 2007. Is there a role for platinum chemotherapy in the treatment of patients with hormone-refractory prostate cancer. Cancer 109, 477–486.

Petros, R.A., Desimone, J.M., 2010. Strategies in the design of nanoparticles for therapeutic applications. Nat. Rev. Drug Discov. 9, 615–627.

Rowinsky, E.K., 2005. Targeted induction of apoptosis in cancer management: the emerging role of tumor necrosis factor-related apoptosis-inducing ligand receptor activating agents. J. Clin. Oncol. 23, 9394–9407.

Sandeep, M., Pandey, A.K., 2014. Cerium oxide nanoparticles induced toxicity in human lung cells: role of ROS mediated DNA damage and apoptosis. BioMed Res. Int., 1–14

Shukla, R., Bansal, V., Chaudhary, M., Basu, A., Bhonde, R.R., Sastry, M., 2005. Biocompatibility of gold nanoparticles and their endocytotic fate inside the cellular compartment: a microscopic overview. Langmuir 21, 10644–10654.

Siegel, R., Desantis, C., Jemal, A., 2014. Colorectal cancer statistics. CA Cancer J. Clin. 64, 104–117.

Sreedevi, B., Suvarchala, G., Philip, G.H., 2014. Morphological and physiological abnormalities during development in zebra fish due to Chlorpyrifos. Indian J. Sci. Res. 5, 1–8.

Stone, V., Donaldson, K., 2006. Nanotoxicology: signs of stress. Nat. Nanotechnol. 1, 23–24.

Tao, W., Jiahui, H., Chang, S., Liang, Z., Yijie, S., 2017. Hyaluronic acid-coated chitosan nanoparticles induce ROS-mediated tumor cell apoptosis an enhance antitumor efficiency by targeted drug delivery via CD44. J. Nanobiotechnol. 15, 7.

Udompornmongkol, P., Chiang, B.H., 2016. Curcumin – loaded polymeric nanoparticles for enhanced anti-colorectal cancer applications. J. Biomater. Appl. 30, 1–10.

Unsoy, G., Yalcin, S., Khodadust, R., Gunduz, G., Gunduz, U., 2012. Synthesis optimization and characterization of chitosan–coated iron oxide nanoparticles produced for biomedical applications. J. Nanopart. Res. 14, 964.

Urakami, S., Shiina, H., Sumura, M., Honda, S., Wake, K., Hiraoka, T., Inoue, S., Ishikawa, N., Igawa, M., 2008. Long-term control or possible cure treatment of stage D2 prostate cancer under chemotherapy using cisplatin and estramustine phosphate followed by maximal androgen blockade. Int. Urol. Nephrol. 40, 365–368.

Valsalam, S., Agastian, P., Arasu, M.V., Al-Dhabi, N.A., Ghilan, A.K.M., Kaviyarasu, K., Ravindran, B., Chang, S.W., Arokiyaraj, S., 2019. Rapid biosynthesis and characterization of silver nanoparticles from the leaf extract of Tropaeolum majus L. and its enhanced in-vitro antibacterial, antifungal, antioxidant and anticancer properties. J. Photochem. Photobiol., B: Biol. 191, 65–74.

Venkatachalam, P., Thiyagarajan, M., Keuk, S.B., Palanivel, V., Byung, T.O., 2016. Antidiabetic potential of bioactive molecules coated chitosan nanoparticles in experimental rats. Int. J. Biol. Macromol. 92, 63–69.

Vivek, R., NipunBabu, V., Thangam, R., Subramanian, K.S., Kannan, S., 2013. pH-responsive drug delivery of chitosan nanoparticles as tamoxifen carriers for effective anti-tumor activity in breast cancer cells. Colloids Surf. B. Biointerf. 111, 117–123.

Vivek, R., Thangam, R., Muthuchelian, K., Gunasekaran, P., Kaveri, K., Kannan, S., 2012. Green biosynthesis of silver nanoparticles from Annona squamosa leaf extract and its in vitro cytotoxic effect on MCF-7 cells. Process Biochem. 47, 2405–2410.

Wang, W., Tong, C., Liu, X., Li, T., Liu, B., Xiong, W., 2015. Preparation and functional characterization of tumor-targeted folic acid-chitosan conjugated nanoparticles loaded with mitoxantrone. J. Cent. South. Univ. 22, 3311–3317.

Wong, R.S.Y., 2011. Apoptosis in cancer: from pathogenesis to treatment. J. Exp. Clin. Canc. Res. 30, 87.

You, Y., Cheng, A.C., Wang, M., Jia, R., Sun, K., Yang, Q., Wu, Y., Zhu, D., Chen, S., Liu, M., Zhao, X., Chen, X., 2017. The suppression of apoptosis by α-herpesvirus. Cell Death Dis. 8, 2749.

Zaman, S., Wang, R., Gandhi, V., 2014. Targeting the apoptosis pathway in hematologic malignancies. Leuk. Lymphoma. 55, 1980–1992.

Zheng, S., Gao, X., Liu, X., Yu, T., Zheng, T., Wang, Y., You, C., 2016. Biodegradable micelles enhance the antiglioma activity of curcumin *in vitro* and *in vivo*. Int. J. Nanomed. 11, 2721.